

Hideki Takebayashi*, Masakazu Moriyama*
Kobe University, Kobe, Japan

1. INTRODUCTION

It is clear that energy consumption in the district heating and cooling (DHC) system is reducible with heat source centralization, recovery of anthropogenic heat and practical use of unused energy, etc., as compared with the heating and cooling system by the individual heat source. Moreover, when utilizing unused energies, such as a sewer, river water, and seawater etc., anthropogenic heat by air conditioning system is emitted out of the area, and it is contributing to curtailment of anthropogenic heat in the area. Therefore, it is predicted that such a DHC system contributes also to curtailment of urban heat island. This research considered influence such a DHC system affects urban heat island using the numerical model, based on the operation data in an actual DHC system in Tokyo region.

2. CALCULATION MODEL

The normal $k-\epsilon$ type model is used for the turbulent flow model. The eddy viscosity coefficients of the vertical direction and the horizontal direction are separated, and dealt with so that the turbulent flow diffusion phenomenon of the vertical direction is fully reflected, Ca (1999). The domain for calculation is Shinjyuku, Tokyo area. They have a 5km x 5km domain centering on Shinjuku high-rise complex. The time for examination is at 3:00 and 15:00 in summer. The domain is divided into a 50m x 50m mesh at equal intervals, and as for the vertical direction, an interval is non-equal mesh system that becomes large, so that it goes upwards. The mesh height near ground surface is 3m. The number of meshes is 100 x 100 x 20.

For inflow boundary conditions, a vertical profile is created using log law based on the weather data observed at the meteorological station. An outflow and upper boundary conditions are free slip conditions. For ground surface boundary conditions, it is necessary to be given the quantity of momentum and sensible heat flux from ground surface. Roughness height that is needed in order to determine quantity of momentum and sensible heat flux is created from the floor area ratio distribution data of the buildings. The number of average stories of the domain for calculation is set as the average value of 0.6m of roughness of the Tokyo area, Kuwagata (1990). In addition, to vegetation, bare soil, water surface, and road surface, 0.5m, 0.01m, 0.001m, and 0.1m is assigned, respectively.

GIS data (detailed numerical value information) is arranged to six classifications, heat budget is solved

**Corresponding author address:* Hideki Takebayashi, Kobe University, Department of Architecture and Civil Engineering, Rokkodai, Nada, Kobe 657-8501, Japan; e-mail: thideki@kobe-u.ac.jp

in each category, and surface temperature is determined according to each category. Convection sensible heat flux from each category surface is estimated by using the area ratio of a category. Six classifications are follows; vegetation, bare soil surface, water surface, wooden housing lots, other building lots, road.

The outlines of heat budget in each category and calculation of convection sensible heat flux are shown in Fig. 1. Where, R: net radiation (W/m^2), V: convection sensible heat flux (W/m^2), IE: latent heat flux (W/m^2), A: conduction heat flux (W/m^2), H: anthropogenic heat release (sensible heat) (W/m^2), and a: area ratio of each category, and θ_s : surface temperature (degree C), θ_{dz} : under ground temperature (degree C). Since the change of water surface temperature during the day is little, it is fixed as 28 degree C.

The weather condition data (solar radiation, wind velocity, cloudiness, water vapor pressure) that are needed for calculation of the heat budget in each category are given from the observation result in the meteorological station. And the heat budget's coefficients (Aledo, evaporation efficiency, thermal conductivity, heat capacity) of each category are given from the reference database. The calculation result of the surface temperature of each category is shown in Fig. 2. The result is averaged every time exception for one month in August 2002. Surface temperature of road is highest through the day. The amplitude of the surface temperature of other building lots with larger heat capacity is smaller than that of the surface temperature of wooden housing lots with smaller heat capacity. The surface temperature distribution of calculation result at 3:00 and 15:00 created from the area ratio of each category is shown in Fig. 3. Surface temperature is higher around Shinjuku in the nighttime, and surface temperature is higher in the area of the housing lots in the west side of calculation domain in the daytime.

For initial conditions, air temperature is uniform to the whole calculation domain, and the vertical profiles of the other parameters are created using log law, as same as inflow boundary conditions.

3. CALCULATION CONDITION

The weather conditions for the calculation are the normal wind condition and the weak wind condition in typical summer fine days. It is thought that the influence of anthropogenic heat release on the air temperature distribution appear notably in the weak wind condition. Extracting the fine day and weak wind condition based on the observation data at the meteorological station in August 2002, boundary condition of the normal wind condition is created from average data of the fine weather day, and boundary

condition of the weak wind condition is selected from the from the typical data of weak wind day.

As conditions for anthropogenic heat release (sensible heat flux), the anthropogenic heat unit (amount of anthropogenic heat generating / heat load) is used as follows; in the non-residential building, for the individual heat source generation case (air conditioning: 1.50, hot-water supply: 0.54), for the DHC case (2.477), for the energy advanced use type DHC case (absorption and boiler system: 2.414, electric system: 1.944), and for the non DHC case (-); and in the residential building, the anthropogenic heat unit is same to the individual heat source case (above shown) for all cases, Agency for Natural Resources and Energy, Japan (2003). It is considered as a total of eight cases to each weather conditions, supposing two patterns of land use, one is present land use and another is urban development progress land use.

Floor area data of 500m mesh data is used for the calculation of the anthropogenic heat release distribution. Anthropogenic heat release distribution at 3:00 is shown in Fig. 4. Anthropogenic heat release in the individual heat source generation case is the largest of all cases, because the anthropogenic heat unit is the smallest of all cases. In the greatest mesh around Shinjuku area, the quantities of the anthropogenic heat release are 96.3W/m^2 for the individual heat source generation case, 77.9W/m^2 for the DHC case, 77.2W/m^2 for the energy advanced use type DHC case, and 54.5W/m^2 for the non DHC case. In the case of urban development progress land use, the amount of anthropogenic heat release also stands in a same line in above order, and the difference of each case is several W/m^2 .

Anthropogenic heat release distribution at 15:00 is shown in Fig. 5. The tendency of a distribution is similar with the distribution at 3:00, and the quantities of the anthropogenic heat release are 967.2W/m^2 , 814.7W/m^2 , 807.1W/m^2 , 431.4W/m^2 , in order of each case in the greatest mesh. In the case of urban development progress land use, the amount of anthropogenic heat release also stands in a same line in above order, and the difference of each case is several dozens W/m^2 .

The discharge height of anthropogenic heat release is shown in Fig. 6. Discharge height is set from the roof of the buildings based on the stories number data of the buildings. The anthropogenic heat release distribution of the road is shown in Fig. 7. The discharge height of anthropogenic heat is set to 1.5m as first cell from ground surface. The anthropogenic heat release distribution of the housing lots at 3:00 and 15:00 are shown in Fig. 8. These values are included also into Fig. 4 and 5. As compared with Figs. 4 and 5 these are smaller values, so the dominant factors of the heat source are office and commercial buildings than the residence.

4. CALCULATION RESULT

4.1 Normal Wind Condition

The calculation results of air temperature

distribution at the height of 1.5m in 8 cases of anthropogenic heat release conditions in the normal wind condition at 3:00 and 15:00 are shown in Figs. 9 and 10. And, the calculation results of air temperature section distribution in the A-A' section (refer to Fig. 9) are shown in Figs. 11 and 12.

The differences of air temperature distributions by the conditions of anthropogenic heat release are very small, and it is difficult to distinguish the difference from the figures. However, the calculation results in the case of non DHC show that air temperature in around Shinjuku is lower than those of other conditions. And, the difference in the thermal boundary layer by the different anthropogenic heat release can be distinguished in air temperature section distribution. Much heat is discharged around Shinjuku and the circumference air temperature is higher.

Air temperature around Shinjuku are not high at 15:00, because the discharge height of anthropogenic heat release of the office and commercial buildings is set from roof top of the building using the database of building height, and surface temperature of other building lots is a little lower than that of wooden housing lots in the daytime. But, because surface temperature is kept to high, air temperature around Shinjuku is high in the nighttime.

4.2 Weak Wind Condition

The calculation results of air temperature distribution at the height of 1.5m in 8 cases of anthropogenic heat release conditions in the weak wind conditions at 3:00 and 15:00 are shown in Figs. 13 and 14. And, the calculation results of air temperature section distribution in the A-A' section are shown in Figs. 15 and 16.

It is difficult to distinguish the difference of air temperature by the conditions of anthropogenic heat release from the figures. Air temperature distribution at 3:00 shows the almost same tendency as the distribution in the normal wind condition. Air temperature at 15:00 around Shinjuku in the normal wind condition is not high, but that in the weak wind condition is high. Air the temperature distribution follows the anthropogenic heat release distribution mostly. In the weak wind condition the discharged heat is seldom spread, so air temperature around Shinjuku is high.

When the individual heat source is replaced with DHC and non DHC, the change of air temperature at 15:00 is shown in Fig. 17 in the weak wind condition. When it replaces with DHC, air temperature in circumference of the discharge point of the individual heat source falls about 1 degree C at the maximum, and air temperature in circumference of the discharge point of anthropogenic heat release is rising about 0.8 degrees C at the maximum by DHC.

5. CONCLUSIONS

The numerical calculations are examined about the urban heat island mitigation effect by spread expansion of the energy advanced use type DHC

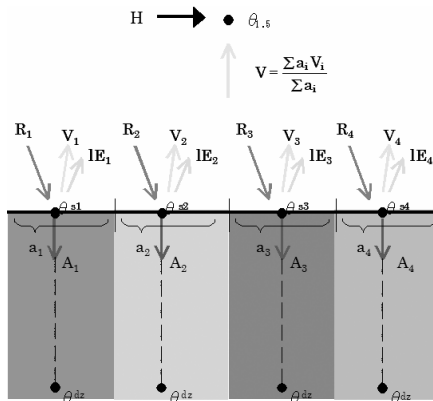
system. Although the influences on air temperature by the conditions of anthropogenic heat release are very small, from the calculation result of air temperature section distribution, the difference in the thermal boundary layer by the different anthropogenic heat release is distinguished.

Acknowledgments

This research was carried out by part of the introductory promotion of the alternative energy etc. by Agency for Natural Resources and Energy, Ministry of Economy, Trade and Industry, Japan.

References

V. Ca, T. Asaeda, Y. Ashie 1999: Development of a numerical model of the urban thermal environment, Journal of Wind Engineering and Industrial Aerodynamics, 81, 181-196
 T. Kuwagata, J. Kondo 1990: Estimation of aerodynamic roughness at the regional meteorological stations (AMeDAS) in the central part of Japan, Tenki, 37.3, 197-201
 Agency for Natural Resources and Energy, Ministry of Economy, Trade and Industry, Japan 2003: Report of basic investigation for the introductory promotion of the alternative energy etc. (in Japanese)



For each category, following formulas are applied

$$R_i = V_i + IE_i + A_i$$

Figure 1 Outlines of heat budget in each category and calculation of convection sensible heat flux

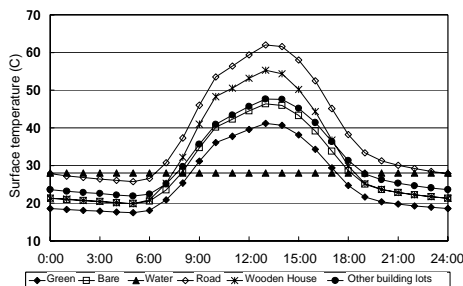


Figure 2 Calculation result of surface temperature of each category

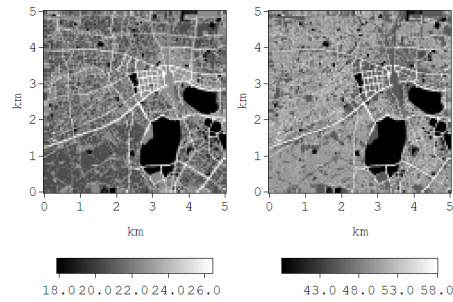


Figure 3 Surface temperature of calculation result at 3:00 (Left) and 15:00 (Right) (degree C)

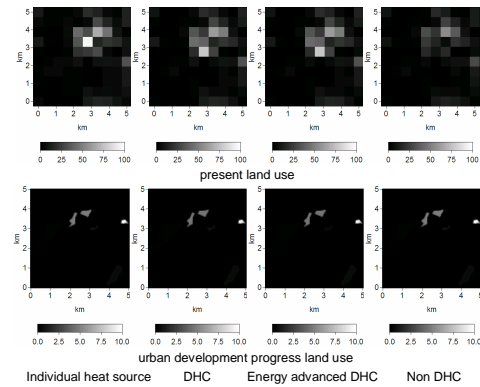


Figure 4 Anthropogenic heat release at 3:00 (W/m²)

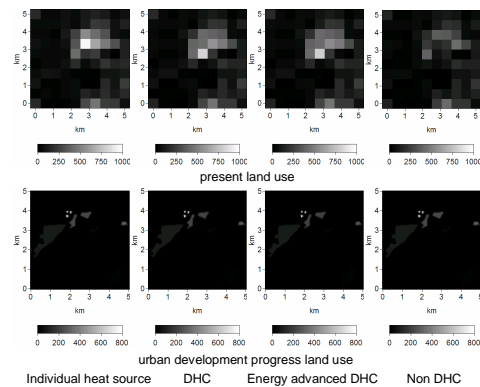


Figure 5 Anthropogenic heat release at 15:00 (W/m²)

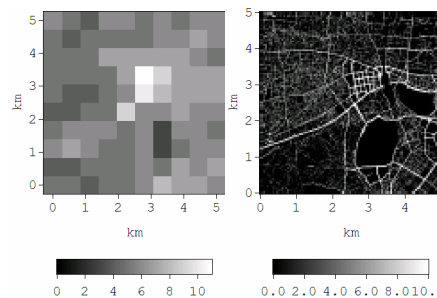


Figure 6 (Left) Discharge height of anthropogenic heat release (mesh number)

Figure 7 (Right) Anthropogenic heat release of road (W/m²)

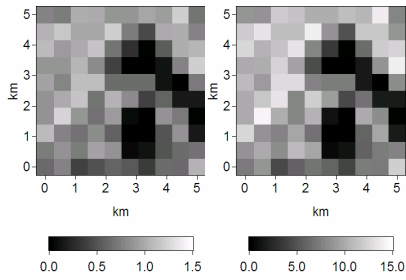


Figure 8 Anthropogenic heat release of housing lots at 3:00 (Left) and 15:00 (Right) (W/m^2)

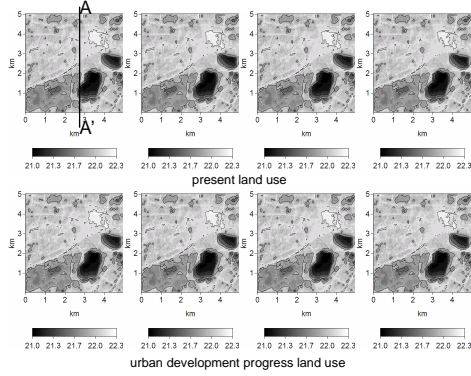


Figure 9 Calculation results of air temperature in the normal wind condition at 3:00 (degree C)

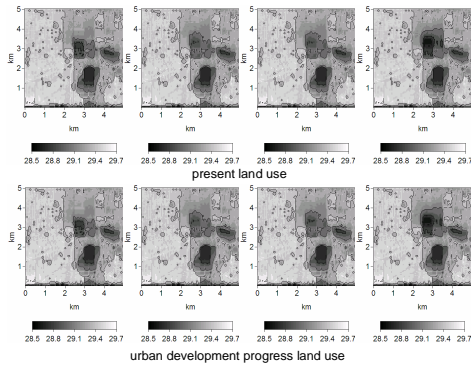


Figure 10 Calculation results of air temperature in the normal wind condition at 15:00 (degree C)

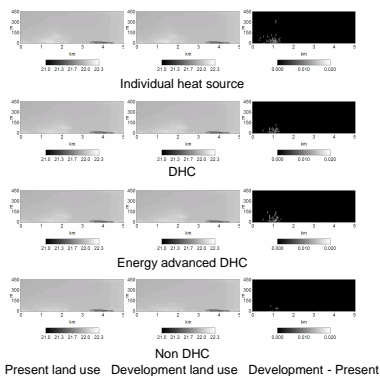


Figure 11 Calculation results of air temperature section in the normal wind at 3:00 (degree C)

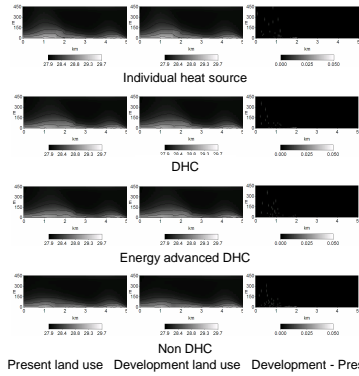


Figure 12 Calculation results of air temperature section in the normal wind at 15:00 (degree C)

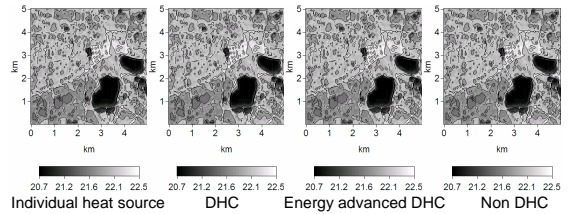


Figure 13 Calculation results of air temperature distribution in the weak wind condition at 3:00 (degree C)

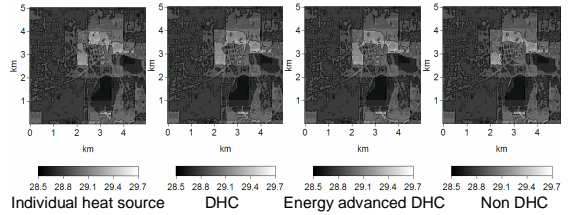


Figure 14 Calculation results of air temperature distribution in the weak wind condition at 15:00 (degree C)

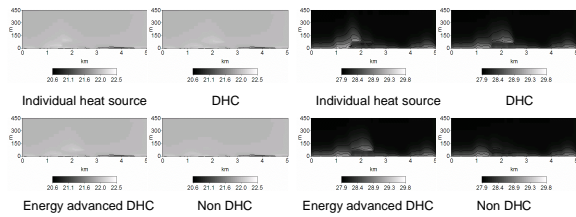


Figure 15 (Left) Calculation results of air temperature section distribution in the weak wind condition at 3:00 (degree C)

Figure 16 (Right) Calculation results of air temperature section distribution in the weak wind condition at 15:00 (degree C)

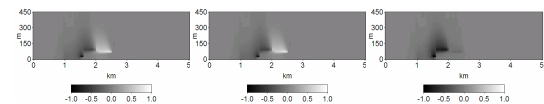


Figure 17 Change of air temperature at 15:00 in the weak wind condition (degree C)